Neoplasia • Vol. 8, No. 1, January 2006, pp. 69–78 69

www.neoplasia.com

Inhibition of Decay-Accelerating Factor (CD55) Attenuates Prostate Cancer Growth and Survival *In Vivo*[1]

Robert D. Loberg[*,†], *LaShon L. Day*[*], *Rodney Dunn*[*], *Linda M. Kalikin*[*] and *Kenneth J. Pienta*[*,†]

[*]Department of Urology, University of Michigan Urology Center, Ann Arbor, MI, USA;
[†]Department of Internal Medicine, University of Michigan, Ann Arbor, MI, USA

Abstract

Decay-accelerating factor (CD55) is a member of membrane-bound complement-regulatory proteins. CD55 expression correlates with poor survival in patients with colorectal cancer and has been implicated in the survival and tumorigenesis of blood-borne malignancies. Histologic analysis of clinical specimens from patients with advanced prostate cancer revealed an increase in CD55 expression in prostate tumor epithelial cells. CD55 was shown to be functionally active and to inhibit complement-mediated lysis in PC-3 and DU145 cells. The percentage of lysis was correlative with the CD55 expression profile observed in these prostate cancer cell lines. These data suggest that CD55 is an important regulator of prostate cancer cell survival. As a result, we have hypothesized that CD55 expression on prostate cancer cells promotes cell survival and contributes to the metastatic potential of prostate cancer cells. To determine the role of CD55 in prostate cancer tumorigenesis and metastasis, we generated PC-3^{Luc} prostate cancer cells with CD55 siRNA-targeted disruption. We found that PC-3^{Luc}/CD55 siRNA constructs in SCID mice resulted in a significant attenuation of overall tumor burden. Further investigation into the mechanisms of CD55-mediated tumor cell/microenvironment interaction is necessary to understand the role of CD55 in tumor cell survival and metastatic lesion formation.
Neoplasia (2006) **8,** 69–78

Keywords: Prostate, cancer, CD55, DAF, complement.

Introduction

Tumorigenesis and metastasis are results of a multistep process that begins with the transformation of cells to an oncogenic phenotype and includes unregulated growth, angiogenesis, breakdown of the extracellular milieu, intravasation, survival in the circulation, adhesion to the target organ endothelium, extravasation, and subsequent growth [1,2]. Each step in this process requires successful immune evasion by disseminated tumor cells in an environment where there are elevated innate immune response and elevated adaptive immune response. The principle of immunologic surveillance suggests that the immune system is constantly monitoring and trying to eradicate abnormal clones recognized by the host immune system as "foreign" bodies. Coley [3] demonstrated evidence for an immune response to tumor cells by reporting spontaneous tumor regression that is associated with bacterial infection. Furthermore, Coley [3] noted a higher incidence of spontaneous tumor development in mice with B-cell or T-cell deficiency and reported that the presence of lymphocytic infiltration in tumors correlates with better prognosis. Historically, cancer patients are known to have elevated circulating tumor-specific $CD8^+$ lymphocytes; recently, we reported an elevation in complement activation in patients with advanced hormone-refractory prostate cancer [4]. Antitumor immunotherapy has demonstrated varying clinical utilities by using tumor vaccines that target tumor-specific antigens (TSAs) and tumor-associated antigens (TAAs) [5–9]. The expression of TSAs and TAAs has been shown to induce the activation of the complement immune system, creating a cytotoxic environment for tumor cell metastasis [10]. The mechanisms adapted by tumor cells that confer resistance to lysis through the homologous complement system may identify novel potential targets for directed therapy.

The complement immune system consists of a series of glycoproteins that participate in an enzymatic cascade, resulting in the formation of membrane attack complex and cell lysis. As a means of host protection against the "bystander killing" effect of activated complements, host cells express membrane-bound complement-regulatory proteins (mCRPs), including a membrane cofactor protein (CD46), a decay-accelerating factor (CD55), and protectin (CD59), all of which inhibit complement-mediated lysis through independent mechanisms [11–13]. Recently, we have demonstrated the overexpression of CD55 in clinical specimens from patients with advanced prostate cancer compared to normal nonmalignant prostate tissues by tissue microarray analysis and real-time polymerase chain reaction

Address all correspondence to: Robert D. Loberg, PhD, University of Michigan Urology Center, 7431 CCGC, 1500 East Medical Center Drive, Ann Arbor, MI 48109-0946.
E-mail: rloberg@umich.edu

[1]This work was supported, in part, by National Cancer Institute grants (SPORE) PO1 and RO1. We would like to thank the AFUD Scholarship Program for supporting R.D.L. as an AFUD scholar.
Received 10 October 2005; Revised 4 November 2005; Accepted 7 November 2005.

DOI 10.1593/neo.05679

(PCR) [14]. CD55 is a glycosylphosphatidylinositol-linked glycoprotein consisting of four SUSHI (SCR) domains in the N-terminal domain and inhibits complement lysis by accelerating the decay of C3 and C5 convertases [15]. An alternative function of CD55 has been proposed when CD55 was identified as a ligand for CD97 and was shown to participate in cell-to-cell/matrix adhesion [16]. CD97 is a member of the epidermal growth factor (EGF)-TM7 family; the binding of CD55 to CD97 has been shown to be Ca^{2+}-dependent and has been implicated in the dedifferentiation of endothelial cells [17]. In this present study, we report that prostate cancer cells upregulate CD55 as a survival mechanism against complement-mediated lysis. Furthermore, we provide evidence to suggest a role for CD55 in prostate cancer cell tumorigenesis and metastasis by siRNA- mediated knockdown CD55 expression in an *in vivo* model of metastasis.

Materials and Methods

Materials

This study used vascular endothelial growth factor (VEGF), tumor necrosis factor α (TNFα), transforming growth factor β (TGFβ), EGF, interleukin (IL) 6, TRAP6 (Sigma-Aldrich, St. Louis, MO), anti-CD55 (clone BRIC 216), rabbit complement (Serotec, Inc., International, Raleigh, NC), anti-endoglin (clone 8E11; Chemicon International, Temecula, CA), Cy5, and calcien AM (Molecular Probes, Inc., Carlsbad, CA); all other reagents were obtained from Sigma-Aldrich.

Cell Culture

Cell lines PC-3, DU145, LNCaP, human microvascular endothelial cells (HMVECs), human bone marrow endothelial (HBME), and RWPE-1 (ATCC, Manassas, VA) were passaged under appropriate growth conditions. PC-3^{Luc} cells were constructed by stably transfecting PC-3 cells with luciferase construct, as previously described [18]. PC-3, DU145, and LNCaP cells were maintained in RPMI 1640 + 10% fetal calf serum (FCS; Invitrogen Corp., Carlsbad, CA), and HBME cells were maintained in DMEM + 10% FCS. HMVECs were maintained in EGM + 5% FCS, and RWPE-1 cells were maintained in KSFM (Invitrogen Corp.). Cells were passaged by trypsinization using 1× trypsin + EDTA (Invitrogen Corp.) and resuspended in appropriate growth media.

Immunoblot Analysis

Cells were lysed in RIPA buffer (50 mM Tris–HCl, pH 7.4, 1% NP-40, 150 mM NaCl, 1 mM EDTA, 1 mM PMSF, 1 mM Na_3VO_4, 1 mM NaF, 1 μM okadaic acid, and 1 μg/ml aprotinin, leupeptin, and pepstatin). Proteins were separated under nonreducing conditions by SDS-PAGE and transferred onto nitrocellulose membrane. Membranes were blocked with 5% milk in TBST (0.1% Tween in TBS) for 1 hour at room temperature. They were incubated overnight at 4°C with primary antibodies: anti-CD55 (clone BRIC 216; Serotec, Inc.) and anti-actin (Cell Signaling, Beverly, MA). Membranes were washed three times prior to incubation with HRP-conjugated secondary antibodies (Cell Signaling) for 1 hour at room temperature. Protein expression was visualized by chemiluminescence (Promega, Madison, WI).

PCR

cDNA was synthesized from 5 μg of total RNA using the First Strand Superscript cDNA synthesis kit (Invitrogen Corp.) following the manufacturer's instructions. Standard PCR techniques were used to detect gene expression. RNA integrity was determined using Agilent technology prior to cDNA synthesis reactions (Agilent, Inc., Palo Alto, CA). Reactions contained 2.5 μl of 10× reaction buffer, 2.5 μl of 2 mM dNTP mix, 1 μl of each primer at 20 pmol/μl, 2 μl of cDNA, 0.5 μl of Taq, and 1.5 μl of 25 mM $MgCl_2$ in a total volume of 25 μl. Gene-specific primers were as follows: CD55 sense 5′-TGATCTGCC-TTAAGGGCAGTCAATGGT-3′ and antisense 5′-TACAATAA-ATAGAGTGCTCTCCAATCA-3′; β-actin sense 5′-CCTCGC-CTTTGCCGATCC-3′ and antisense 5′-GGATCTTCATGA-GGTAGTCAGTC-3′. Amplification was performed as follows: 94°C (2 minutes), 94°C (30 seconds), 52°C (30 seconds), and 72°C (1 minute) at 25, 30, and 35 cycles. Amplification products were separated on a 1% agarose gel in 1× TBE and visualized with ethidium bromide staining. For real-time PCR experiments, primers and probes were purchased from ABI, Inc. Assays on Demand (Foster City, CA). GAPDH was used as an internal control. Samples were run in replicates of four and normalized to the respective GAPDH levels, as previously described [19].

Flow Cytometry

Cells were grown to 75% to 80% confluency and collected by trypsinization with 1× trypsin/EDTA. Cells were washed twice with PBS, centrifuged, and resuspended at 5×10^5 cells/ml. Primary antibodies were diluted in PBS at 1:1000 and mixed by inversion. Primary antibodies were added to each sample and incubated by rocking at 4°C for 1 hour. After primary incubation, PBS was added to each sample and mixed by inversion. Samples were centrifuged, and the supernatant was discarded. Secondary antibody (Cy-5) was added to each sample and placed at a temperature of 4°C for 30 minutes. After secondary antibody incubation, samples were washed with 1 ml of PBS and centrifuged at 2000*g* for 5 minutes. The supernatant was discarded, samples were resuspended in 3.7% paraformaldehyde (in PBS), and transferred to flow cytometry tubes for analysis by the Flow Cytometry Core at the University of Michigan (Ann Arbor, MI).

Cell-to-Cell Adhesion

HMVECs or HBME cells were plated at 5×10^4 cells/ml in 96-well plates and allowed to grow for 4 days at 37°C in 5% CO_2, or until they have formed 90% to 100% confluent monolayers. PC-3, DU145, and LNCaP cells were serum-starved for 2 hours in SFM-RPMI and released with 0.5 mM EDTA-HBSS for 1 hour at room temperature. PC-3, DU145, and LNCaP were resuspended in RPMI-SFM media at 1×10^6 cells/ml in PBS. PC-3, DU145, and LNCaP were labeled with CONC calcein AM, washed with PBS, and resuspended in SFM-RPMI with or without anti-CD55 blocking antibody at 2×10^5 cells/ml. A total of 2×10^4 labeled PC-3, DU145, or LNCaP

cells were added to confluent HMVECs or HBME cells and incubated for 45 minutes at 37°C in 5% CO_2. Cells were then gently washed with DPBS thrice, and absorbance was read on a microtiter plate reader at 490 nm excitation and 530 nm emission.

Complement-Mediated Lysis Assay

Cells were plated in a 96-well plate at 5×10^4 cells/ml and grown to confluence. Cells were washed twice with serum-free RPMI 1640 + 1% bovine serum albumin (BSA) and incubated with calcein AM (5 μg/ml) for 30 minutes at 37°C. Cells were washed twice with RPMI + 1% BSA prior to opsonization with anti-endoglin MJ7/18 antibody (Chemicon International) for 1 hour at 37°C. Cells were incubated in the presence of 10% baby rabbit complement (Serotec, Inc.) in RMPI + 1% BSA for 45 minutes at 37°C. The supernatant was transferred to a new 96-well plate and represented the "complement-mediated release" calcein AM fraction. The calcein AM remaining in the cells was released by incubation with RPMI + 1% BSA + 0.1% Triton X-100 for 15 minutes at room temperature. Lysates were then transferred to a 96-well plate, the calcein AM was released by complement, and detergent was quantified using a VersaMax (Molecular Devices, Sunnyvale, CA) fluorescence plate reader. The percentage of specific lysis was calculated as complement-mediated release/maximal release multiplied by 100%, where maximal release is the complement-mediated release plus the detergent-mediated release of calcein AM.

CD55 Deposition into the Extracellular Matrix

Cells were plated in a 96-well plate at 5×10^4 cells/ml and allowed to grow for 14 hours. Cells were then stimulated with the indicated growth factors for 24 hours in serum-free media. Cells were released with 0.02% EDTA at 37°C for 60 minutes. The absence of cells was confirmed by light microscopy, and wells were washed six times with PBS. PBS + 0.05% Tween 20 was added to each well for 30 minutes at 4°C to block nonspecific binding of antibodies. Anti-CD55 (BRIC 216) primary antibody was added to each well (10 μg/ml in PBS + 0.05% Tween 20) for 1 hour at 4°C. Wells were washed thrice with PBS + 0.05% Tween 20, and an anti-mouse fluorescein isothiocyanate secondary antibody was added to the wells for 1 hour at 4°C. Wells were then washed six times with PBS + 0.05% Tween 20. ABTS mixture was prepared fresh (0.2 M dibasic sodium phosphate and 0.1 M citric acid, pH 5.0), and 30% H_2O_2 was added to the ABTS solution immediately prior to use. The ABTS mixture was added to each well and read on a microplate reader at 405 nm within 30 minutes.

CD55 siRNA Knockdown in PC-3 Cells

DNA oligos for siRNA-targeted disruption of CD55 were designed using sequences obtained from Ambion, Inc. (Austin, TX). Sense and antisense sequences were annealed in 1× annealing buffer and ligated into pSilencer (Ambion, Inc.). Ligations consisting of 1 μl of annealed oligos (8 ng/μl) and 1 μl of linearized pSilencer (0.1 mg/ml) were incubated at 24°C for 1 hour in the presence of 5 U of T4 DNA ligase in 1× T4 DNA ligase buffer (Invitrogen, Inc., Carlsbad, CA) following the manufacturer's instructions. pSilencer containing GAPDH was used as control for PC-3^{Luc} transfection, and pSilencer containing Scrambled oligos was used as control for siRNA-mediated knockdown.

Bioluminescent In Vivo *Model of Metastasis*

Bioluminescent imaging of PC-3^{Luc} was preformed, as previously described, through The University of Michigan Small Animal Imaging Resource facility [18]. Briefly, PC-3^{Luc} cells containing CD55 siRNA or Scrambled siRNA were introduced into male SCID mice (5–6 weeks) by intracardiac injections. Mice were serially imaged weekly for 7 weeks using a charge-coupled device (CCD) IVIS system using a 50-mm lens (Xenogen Corp., Alameda, CA), and the results were analyzed using LivingImage software (Xenogen Corp.). Mice were intraperitoneally injected with luciferin (40 mg/ml), and ventral images were acquired 15 minutes postinjection under 1.75% isoflurane/air anesthesia. The total tumor burden of each animal was calculated using regions of interest (ROIs) that encompassed the entire animal. Animals were sacrificed after week 7 image, and individual organs were harvested and placed in formalin.

Histology

Animals were sacrificed, and tissue specimens were fixed in formalin for hematoxylin and eosin histologic analysis following routine protocols. Tibias were decalcified in a Cal-Ex II (Fisher Scientific, Hampton, NH) decalcifying solution for 24 to 48 hours, and 5-μm sections were placed on uncharged glass slides. Anti-luciferase (1:3200; Sigma, St. Louis, MO) antibodies with EnVision Rabbit Peroxidase Kit (DAKO Corp., Carpinteria, CA) were used to confirm the presence of PC-3^{Luc} cells within tumors.

Statistics

Data were analyzed with GraphPad (San Diego, CA) Prism software. A one-way ANOVA was used with Bonferroni's post hoc analysis for comparisons between multiple groups. A Student's *t* test was used for comparisons between two groups. Significance was defined as $P < .05$. For analysis of *in vivo* bioluminescent experiments, a mixed regression model was used to determine the differences in growth rate and initial value between the $CD55^+$ and $CD55^-$ groups. Growth rate was explored both as a quadratic (curved) effect and as a linear effect. Interactions were used between growth rate and group indicator ($CD55^+$ *versus* $CD55^-$) variables to determine whether shape and rate differed by group. A backward model building selection was used to arrive at the most parsimonious model. All tests were performed at the 5% significance level using the SAS System (SAS, Cary, NC).

Results

Previously, we have demonstrated the upregulation of CD55 expression in prostate cancer by tissue microarray analysis [4]. To confirm the presence and overexpression of CD55 in PC-3, DU145, and LNCaP cells, CD55 expression was determined by real-time PCR (Figure 1*A*) and flow cytometry (Figure 1, *B* and *C*) and compared to RWPE-1 cells. Flow

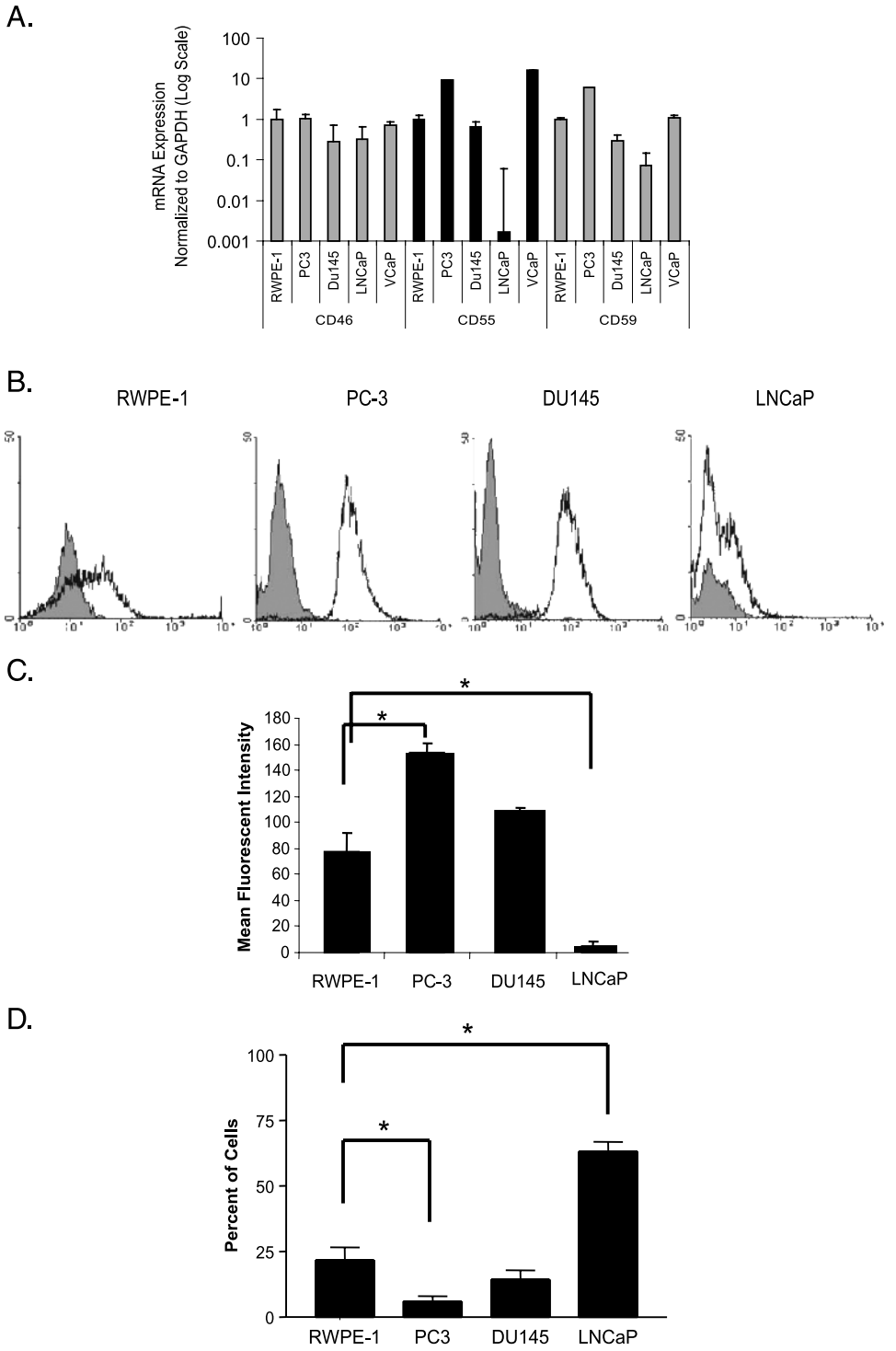

Figure 1. *CD55 and CD97 expression in prostate cancer cell lines. (A) Real-time PCR of CD46, CD55, and CD59 in RWPE-1, PC-3, DU145, and LNCaP cell lines. Each sample was run in quadruplicate and normalized to cell-specific GAPDH quantification. Results are expressed as fold expression of the RWPE-1 cells on a log scale. (B) The protein expression of CD55 was performed in triplicate by flow cytometric analysis. (C) Graphic analysis of the mean fluorescent intensity was normalized to RWPE-1 for each replicate and graphed as mean ± standard deviation. (*significance compared to RWPE-1, P < .01; #significance compared to PC-3, P < .001). (D) Effect of CD55 expression on prostate cancer cell sensitivity to complement lysis. The sensitivity of RWPE-1, PC-3, DU145, and LNCaP cells to complement-mediated lysis was assessed. Lysis assays were performed in triplicate, and percent lysis was calculated: (calcein AM fluorescence from the supernatant/maximal calcein AM fluorescence) × 100.*

cytometric analysis revealed a significant increase in the expression of CD55 on PC-3 and DU145, but not in LNCaP (RWPE-1: 76.88 ± 15.44; PC-3: 153.0 ± 7.49; DU145: 108.5 ± 3.18; LNCaP: 4.61 ± 3.29) (Figure 1*C*). To determine if the expression of CD55 correlated with the resistance to complement-mediated lysis, RWPE-1, PC-3, DU145, and LNCaP cells were incubated in the presence of activated baby rabbit complement and the percentage of lysed cells was

calculated. PC-3 cells demonstrated the greatest resistance to complement-mediated lysis, whereas LNCaP cells were the most sensitive (PC-3: 6.045 ± 1.94; DU145: 14.30 ± 3.57; LNCaP: 63.24 ± 3.6; HMVEC: 13.69 ± 3.53) (Figure 1*D*). From these data, the expression of CD55 correlated with the sensitivity of individual prostate cancer cell lines to complement-mediated lysis and demonstrated that CD55 is present and functional in prostate cancer cells *in vitro*.

Recently, a role for CD55 in adhesion to endothelial cells has been suggested [20]; therefore, we examined the contribution of CD55 in prostate cancer cell adhesion to endothelial cells. PC-3, DU145, and LNCaP cells were incubated on a confluent layer of HMVECs in the absence or presence of an anti-CD55 blocking antibody, and the percentage of cells that adhered was quantified. Inhibition of CD55 attenuated PC-3 cell and DU145 cell adhesion to endothelial cells (Figure 2, *A* and *B*). LNCaP cells did not adhere well to endothelial cells, and inhibition of CD55 did not affect LNCaP adhesion to HMVECs (Figure 2*C*). Previously, preferential adhesion of prostate cancer cells to bone marrow endothelium has been demonstrated [21]; therefore, we determined the role of CD55 in PC-3 adhesion specifically to HBME cells.

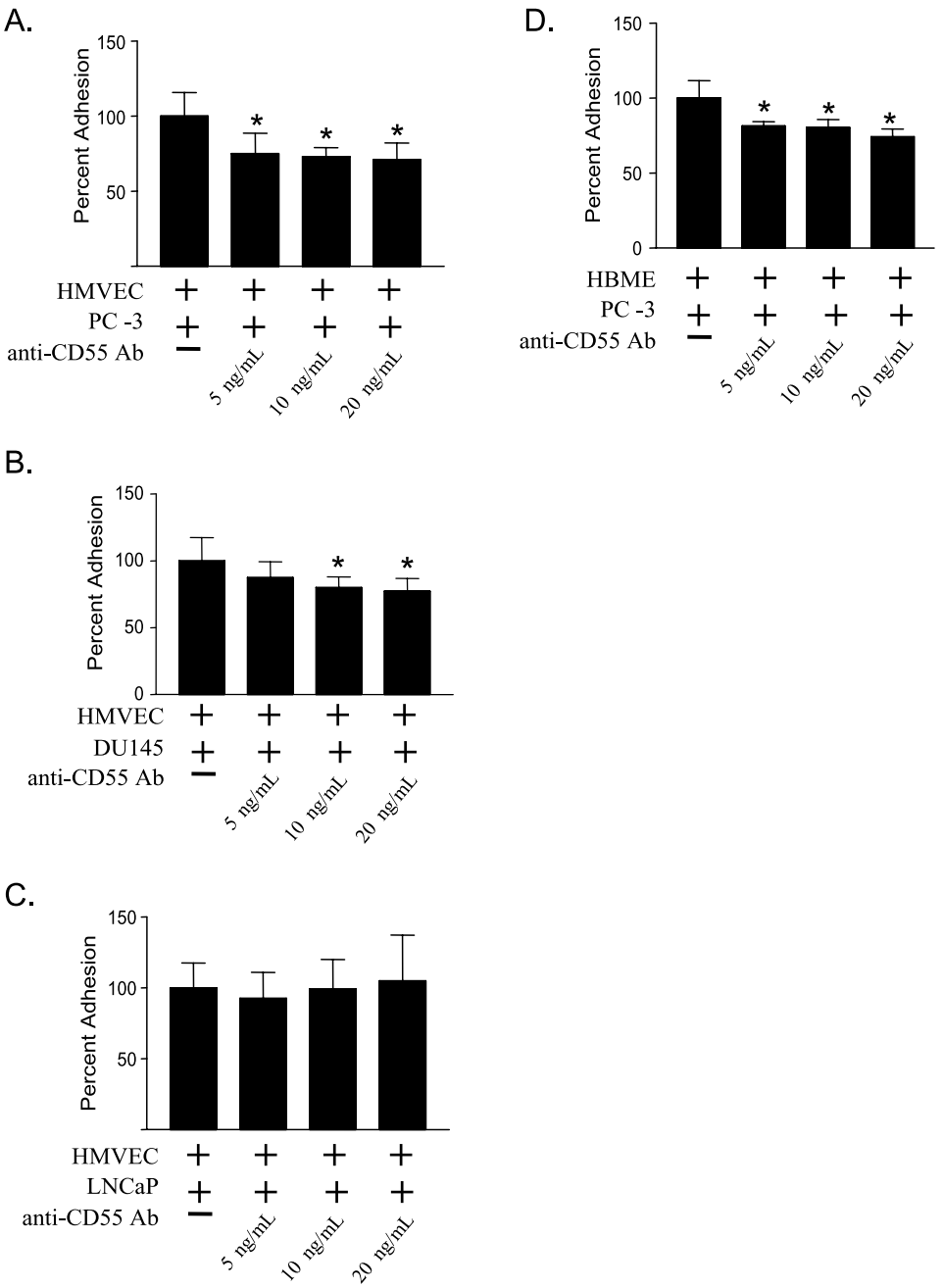

Figure 2. *Inhibition of CD55 attenuates PC-3 cell adhesion to endothelial cells. (A) PC-3, (B) DU145, and (C) LNCaP adhesion to HMVECs was determined in the presence of an anti-CD55 blocking antibody. Cells were treated with anti-CD55 antibody at 5, 10, and 20 ng/ml during the 30-minute adhesion assay. (D) PC-3 cell adhesion to HBME cells was similarly assessed. Results were normalized to untreated cells and expressed as percent adhesion above control. Analysis was performed in triplicate, and the data are presented as mean ± standard deviation (*P < .05).*

Inhibition of CD55 attenuated PC-3 cell adhesion to HBME cells, similar to that observed using HMVECs (Figure 2*D*).

CD55 has been shown to be deposited in the tumor microenvironment and to contribute to metastasis [22,23]. Analysis of CD55 mRNA expression after growth factor stimulation revealed an increase in CD55 mRNA expression mediated by VEGF, TNFα, and EGF (Figure 3, *A* and *B*). Growth factor stimulation of PC-3 cells did not alter CD55 protein expression (data not shown). Therefore, we analyzed the ability of PC-3 to release and secrete soluble CD55 (sCD55) into the extracellular matrix using a matrix deposition assay. To determine the ability of PC-3 and DU145 cells to deposit sCD55 into the extracellular matrix, cells were stimulated with VEGF, TNFα, TGFβ, EGF, and IL-6 for 24 hours, and the amount of sCD55 deposited into the matrix was quantified. PC-3 cells treated with VEGF, TNFα, and EGF had a significant increase in the amount of sCD55 deposited in the matrix (fold expression: VEGF: 8.787 ± 4.438; TNFα: 7.321 ± 3.407; EGF: 13.75 ± 2.555) (Figure 3*C*). Similarly, DU145 cells treated with VEGF, TNFα, and EGF had a significant increase in sCD55 deposition (fold expression: VEGF: 12.21 ± 3.938; TNFα: 13.95 ± 4.846; EGF: 16.28 ± 0.9736) (data not shown).

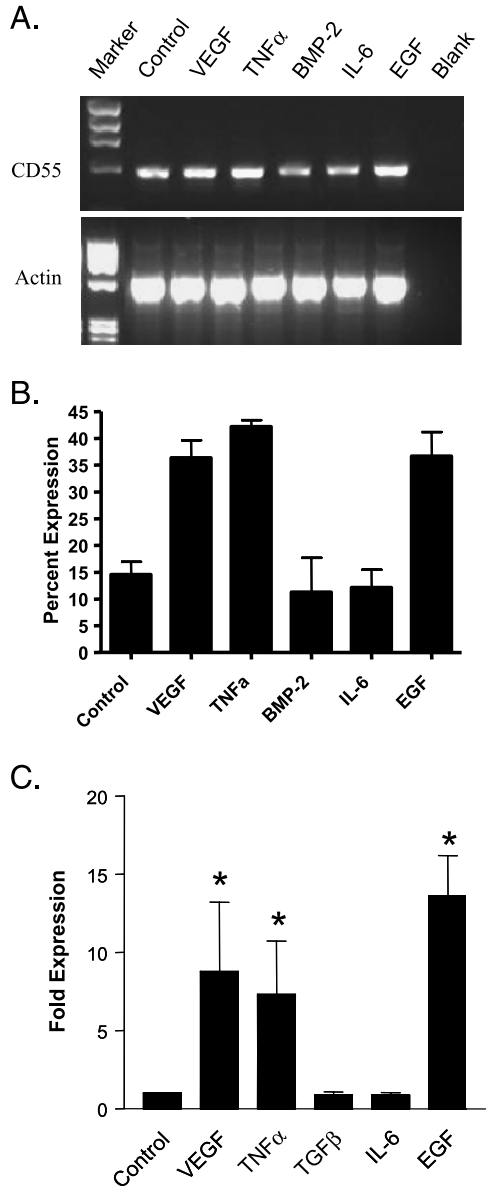

Figure 3. *Growth factor stimulation of PC-3 cells induces CD55 deposition. (A) PC-3 cells were stimulated with VEGF (50 ng/ml), TNFα (50 ng/ml), BMP-2 (50 ng/ml), IL-6 (50 ng/ml), or EGF (50 ng/ml) for 24 hours. CD55 mRNA expression was analyzed by PCR, and β-actin was assessed as control. (B) CD55 protein expression was assessed in total cell lysates by Western blot analysis after stimulation with VEGF (50 ng/ml), TNFα (50 ng/ml), IL-6 (50 ng/ml), or EGF (50 ng/ml) for 24 hours. (C) Soluble CD55 deposition into the extracellular matrix was assessed in PC-3 cells treated with VEGF (50 ng/ml), TNFα (50 ng/ml), TGFβ (50 ng/ml), EGF (50 ng/ml), and IL-6 (50 ng/ml) for 24 hours. Data are presented as mean ± standard deviation (*P < .01).*

To visualize the role of CD55 in prostate cancer metastasis in an *in vivo* mouse model of metastasis, PC-3^{Luc} cells were stably transfected with siRNA constructs targeting CD55 and decreased its expression. Three siRNA sequences targeting distinct regions of the *CD55* gene were used (CD55-1, CD55-2, and CD55-3). We used an siRNA construct containing Scrambled siRNA (Scrambled) as negative control. Comparative analysis of CD55 knockdown between independent siRNA constructs was confirmed by PCR analysis of CD55 expression. Increasing amplifications revealed a decrease in CD55 expression by the CD55-3 siRNA construct compared to the GAPDH- and CD55-1–expressing cells (Figure 4*A*). Decreased CD55 protein expression by CD55-3 construct was further confirmed by Western blot analysis (Figure 4*B*). Furthermore, siRNA-mediated disruption of CD55 was shown to increase the sensitivity of PC-3^{Luc} cells to complement-mediated lysis (Figure 4*C*). Additionally, decreased expression of CD55 did not alter PC-3^{Luc} cell growth in cultures (Figure 4*D*).

To visualize the effects of CD55 knockdown on PC-3^{Luc} tumor growth in an *in vivo* model of metastasis, male SCID mice (5–6 weeks old) received intracardiac injections of PC-3^{Luc} Scrambled cells (n = 10) and PC-3^{Luc} CD55-3 cells (n = 10), and tumor growth was monitored weekly using a CCD camera (Figure 5*A*). A week 1 postinjection of all mice demonstrated at least one focal point of photon emission. Serial bioluminescent images were taken weekly for 6 weeks. During the 6-week period, two mice with PC-3^{Luc} Scrambled cells and three mice with PC-3^{Luc} CD55-3 cells expired spontaneously. On day 45, final images were acquired, and the total tumor burden per animal was quantified. The total tumor burden of mice injected with PC-3^{Luc} CD55-3 was significantly decreased compared to the mice injected with PC-3^{Luc} Scrambled cells (Scrambled: $1.29 \times 10^8 \pm 3.2 \times 10^7$; CD55-3: $3.14 \times 10^7 \pm 7.28 \times 10^6$; mean ± SEM) (Figure 5*B*). To confirm the presence of tumors, histologic sections were analyzed by hematoxylin and eosin staining and revealed tumor infiltration in both soft tissue (data not shown) and osseous metastasis (Figure 5, *C*, *D* and *F*, *G*). Further histologic examination of tibial lesions revealed PC-3^{Luc}–based tumors staining positive for luciferase (Figure 5, *E* and *H*).

Discussion

CD55 is known to be cytoprotective against complement-mediated lysis; however, little is known regarding the role of

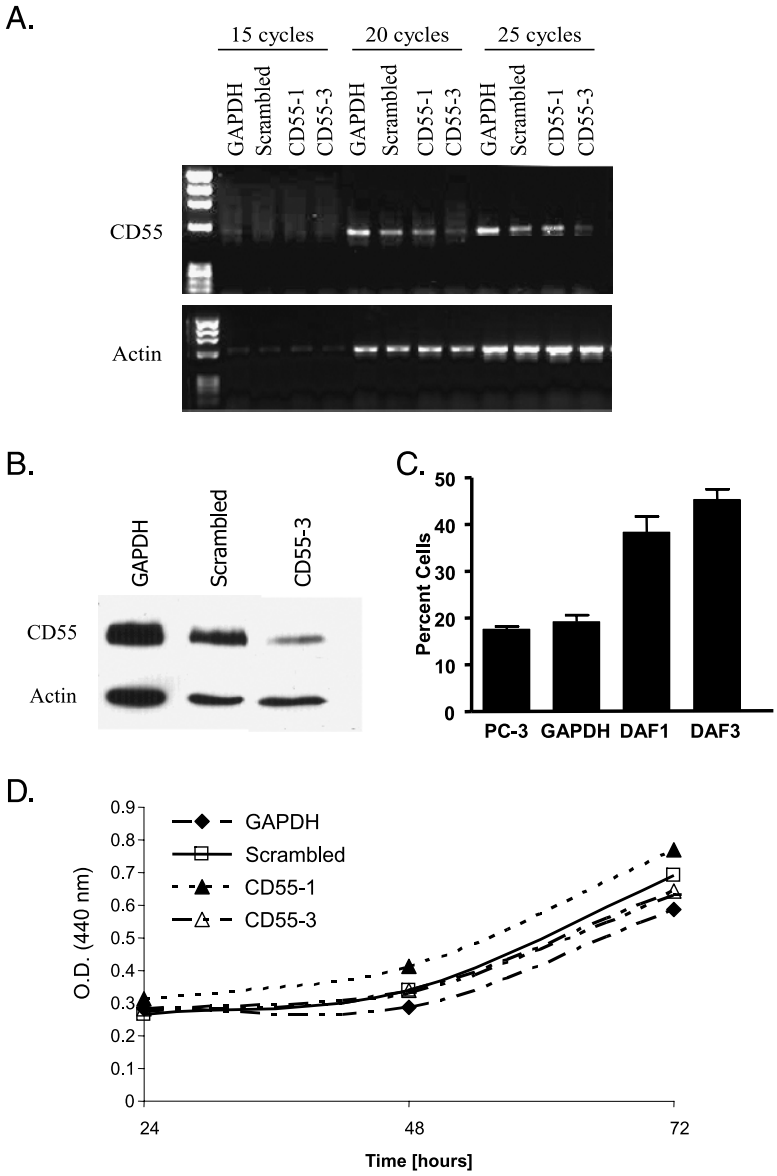

Figure 4. *siRNA-mediated knockdown CD55 expression in PC-3^{Luc} cells. (A) CD55 mRNA expression was visualized in PC-3^{Luc} cells stably expressing CD55 siRNA pSilencer constructs targeting unique regions of the CD55 gene (CD55-1 and CD55-3). GAPDH pSilencer construct was used as transfection control, and pSilencer containing Scrambled siRNA was used as siRNA control. Increasing cycles (15, 20, and 25 cycles) were used to assess CD55 mRNA expression, whereas β-actin analysis was used as control for PCR amplification. (B) CD55 protein expression was visualized by Western blot analysis in the GAPDH, Scrambled, and CD55-3 siRNA PC-3^{Luc} cells. (C) The effect of CD55 knockdown expression on PC-3 cell sensitivity to complement lysis was determined. (D) Proliferation rates of PC-3^{Luc} cells were assessed over a 48-hour period using WST-1 proliferation assay.*

CD55 in prostate cancer survival and metastasis. We have shown that CD55 expression was significantly elevated in PC-3 and DU145 cells, whereas LNCaP cells demonstrated a significantly lower expression (Figure 1). Additionally, resistance to complement-mediated lysis in RWPE-1, PC-3, DU145, and LNCaP cells correlated with differential expression of CD55, indicating a functional role in acquired resistance and promoting prostate cancer cell survival during tumorigenesis, circulation, and metastasis. RWPE-1 cells were used as a reference cell line to compare the role of CD55 expression on prostate cancer cell survival and metastasis. Sensitivity to complement-mediated lysis correlated with increased expression of CD55 on PC-3 and DU145 cells. The fact that LNCaP cells express extremely low levels of CD55 is unclear and may be a result of the cell line being derived from lymph node metastasis compared to the bone and dura microenvironment for PC-3 and DU145 cells, respectively. Future experiments looking at the role of androgens and androgen receptor activation in regulating CD55 expression and activity may be important in delineating the differential expression of CD55 in various prostate cancer cell lines and clinical samples.

The regulation of CD55 expression on endothelial cells has been shown to be a function of bFGF and VEGF stimulation [24,25]. Additionally, colonic cancer cells have demonstrated an increase in CD55 expression in response to EGF stimulation, which is dependent on MAPK signaling [26]. To further understand the mechanisms of CD55-regulated expression in prostate cancer, we stimulated PC-3 and DU145

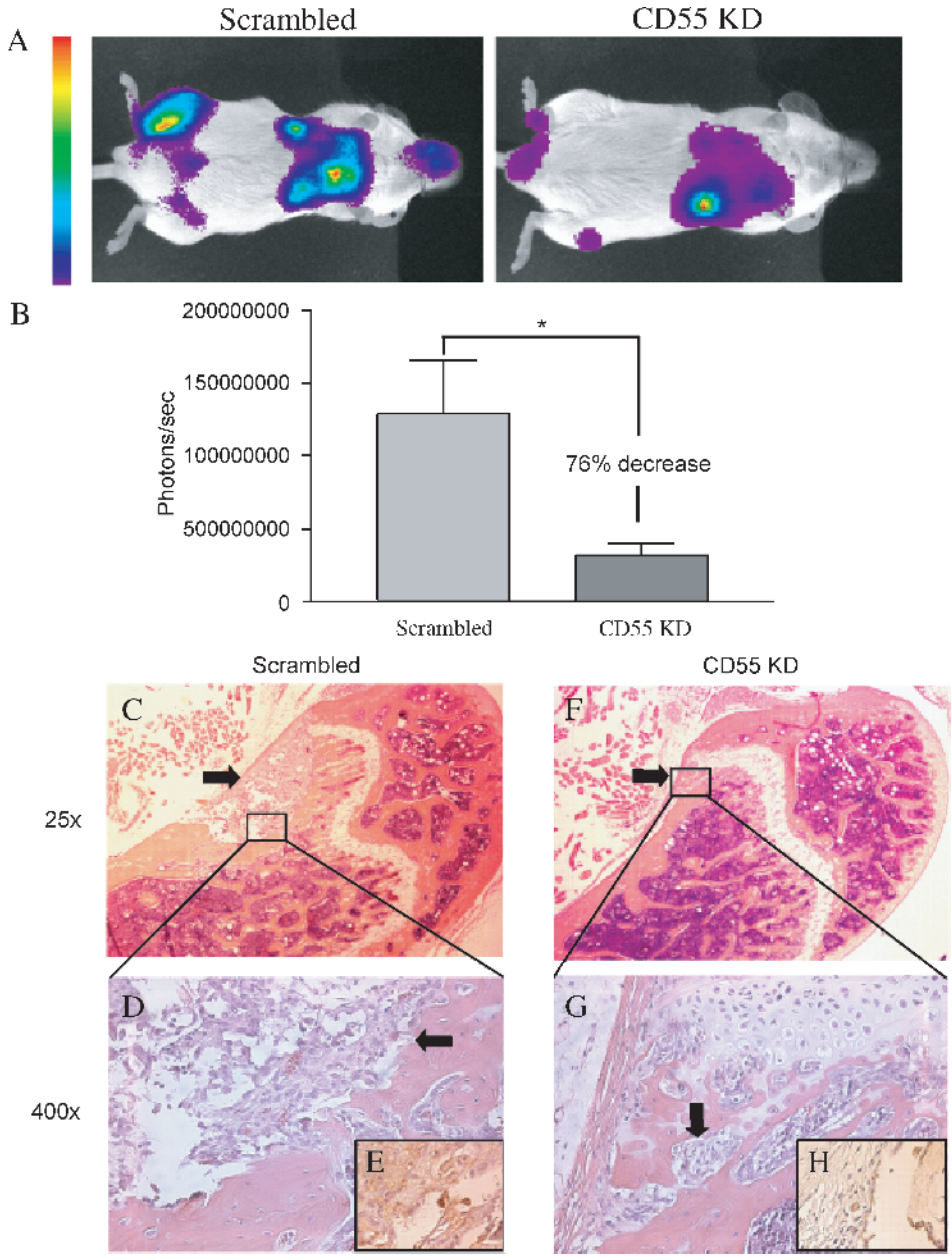

Figure 5. *Downregulation of CD55 reduces total tumor burden* in vivo. *PC-3^{Luc} cells containing either Scrambled siRNA or CD55-3 siRNA constructs were introduced to male SCID mice by intracardiac injection, and tumor volume was monitored over 45 days by bioluminescent imaging (A). Day 45 total tumor burden was measured by ROI quantification of photons-per-second emission from mice injected intraperitoneally with luciferin (B). Histologic analysis of tibial lesions by hematoxylin and eosin staining with ×25 objective (C and F) and ×400 objective (D and G). Arrows indicate the presence of tumor cells in representative sections. Immunohistochemical analysis with anti-luciferase antibodies (E and H) was used to confirm the PC-3^{Luc} cell origin of tumors.*

cells with VEGF, TNFα, TGFβ, IL-6, and EGF and demonstrated that VEGF, TNFα, and EGF induced an increase in sCD55 being released into the surrounding matrix. The presence of CD55 in the tumor microenvironment is currently not understood; however, it may play an important role in protecting cancer cells as they seed a metastatic site and progress to a more aggressive phenotype.

In this present study, we demonstrate for the first time that inhibition of CD55 using siRNA-mediated knockdown expression resulted in a 76% decrease in overall tumor burden after 45 days in a bioluminescent mouse model of metastasis (Figure 5*B*). There was no apparent effect of the number of metastatic lesions or the initial rate of PC-3^{Luc} cell seeding between the CD55 knockdown PC-3^{Luc} cell line and the Scrambled negative control (data not shown). These data indicate a decrease in the ability of PC-3^{Luc} cells deficient in CD55 to successfully grow at a metastatic site and suggest an important role for CD55 in prostate cancer growth and survival.

The complement immune system is activated during various malignancies, including colorectal and prostate cancers [14,27–29]. Tumor cells have been shown to increase complement activation, resulting in the deposition of C3 and C4 in breast cancer and papillary thyroid carcinoma [28,30,31]. In

response to elevated complement activity, cancer cells have developed a mechanism of protection for survival by upregulating mCRP expression [32]. Several studies have shown certain malignancies presenting varying complement activities and tumor cells having varying resistance to complement-mediated lysis [11,32,33]. Varying resistance to the complement system is most likely due to differentially expressed mCRPs within a tumor and between cancers. Expression of mCRPs has been demonstrated in breast cancer, gastric cancer, colorectal cancer, and leukemia and is variable between cancer and within tumors [13,29,31,33–35]. CD55, specifically, has been implicated in tumorigenesis in colorectal cancer. Reports have demonstrated the overexpression of CD55 in colorectal cancer specimens compared to normal results from patients' histology samples and LS174T cells (a colon carcinoma cell line) [36].

Tumor cells have developed several escape mechanisms utilized to promote tumorigenesis and metastasis. Tumor cells are known to downregulate tumor antigens [37], express molecules that inhibit T-cell viability and expansion [B7-H (PDL1 and PDL2) and indoleamine 2,3-dioxygenase] [38–40], and to develop resistance to NK, $CD8^+$ T-cell granzymes, and perforin [41,42]. In this study, we present data demonstrating that the inhibition of complement-mediated lysis by the upregulation of CD55 protects PCa cells and promotes prostate cancer tumorigenesis and metastasis. Further studies are required to further understand the role of CD55 in tumor cell biology and its potential for targeted therapy; however, evidence presented here implicates CD55 as an important mediator of prostate cancer cell survival and tumor growth.

Acknowledgement

We acknowledge the Tissue Core at the University of Michigan.

References

[1] Cooper CR, Chay CH, Gendernalik JD, Lee HL, Bhatia J, Taichman RS, McCauley LK, Keller ET, and Pienta KJ (2003). Stromal factors involved in prostate carcinoma metastasis to bone. *Cancer* **97,** 739–747.

[2] Keller ET and Brown J (2004). Prostate cancer bone metastases promote both osteolytic and osteoblastic activity. *J Cell Biochem* **91,** 718–729.

[3] Coley WB (1991). The treatment of malignant tumors by repeated inoculations of erysipelas. With a report of ten original cases, 1893. *Clin Orthop Relat Res*, 3–11.

[4] Loberg RD (2005). Analysis of membrane-bound complement regulatory proteins in prostate cancer. *Urology* (in press).

[5] Zusman I (1998). Comparative anticancer effects of vaccination and dietary factors on experimentally-induced cancers. *In Vivo* **12,** 675–689.

[6] Hadden JW (1999). The immunology and immunotherapy of breast cancer: an update. *Int J Immunopharmacol* **21,** 79–101.

[7] Schlom J, Tsang KY, Kantor JA, Abrams SI, Zaremba S, Greiner J, and Hodge JW (1999). Strategies in the development of recombinant vaccines for colon cancer. *Semin Oncol* **26,** 672–682.

[8] Rafii S (2002). Vaccination against tumor neovascularization: promise and reality. *Cancer Cell* **2,** 429–431.

[9] Hurwitz AA, Yanover P, Markowitz M, Allison JP, and Kwon ED (2003). Prostate cancer: advances in immunotherapy. *BioDrugs* **17,** 131–138.

[10] Gil J, Alvarez R, Vinuela JE, Ruiz de Morales JG, Bustos A, De la Concha EG, and Subiza JL (1990). Inhibition of *in vivo* tumor growth by a monoclonal IgM antibody recognizing tumor cell surface carbohydrates. *Cancer Res* **50,** 7301–7306.

[11] Gelderman KA, Blok VT, Fleuren GJ, and Gorter A (2002). The inhibitory effect of CD46, CD55, and CD59 on complement activation after immunotherapeutic treatment of cervical carcinoma cells with monoclonal antibodies or bispecific monoclonal antibodies. *Lab Invest* **82,** 483–493.

[12] Wojnicz D, Bar J, and Jankowski S (2002). The role of membrane glycoproteins CD46, CD55 and CD59 in protection of tumor cells against complement lysis. *Postepy Hig Med Dosw* **56,** 603–616.

[13] Thorsteinsson L, O'Dowd GM, Harrington PM, and Johnson PM (1998). The complement regulatory proteins CD46 and CD59, but not CD55, are highly expressed by glandular epithelium of human breast and colorectal tumour tissues. *APMIS* **106,** 869–878.

[14] Loberg R, Day L, and Pienta K (2005). Abstract: the role of CD55 in prostate cancer bone specific metastasis. *Keystone Symp*.

[15] Bjorge L, Jensen TS, and Matre R (1996). Characterisation of the complement-regulatory proteins decay-accelerating factor (DAF, CD55) and membrane cofactor protein (MCP, CD46) on a human colonic adenocarcinoma cell line. *Cancer Immunol Immunother* **42,** 185–192.

[16] Hamann J, Vogel B, van Schijndel GM, and van Lier RA (1996). The seven-span transmembrane receptor CD97 has a cellular ligand (CD55, DAF). *J Exp Med* **184,** 1185–1189.

[17] Hamann J, Stortelers C, Kiss-Toth E, Vogel B, Eichler W, and van Lier RA (1998). Characterization of the CD55 (DAF)–binding site on the seven-span transmembrane receptor CD97. *Eur J Immunol* **28,** 1701–1707.

[18] Kalikin LM, Schneider A, Thakur MA, Fridman Y, Griffin LB, Dunn RL, Rosol TJ, Shah RB, Rehemtulla A, McCauley LK, et al. (2003). *In vivo* visualization of metastatic prostate cancer and quantitation of disease progression in immunocompromised mice. *Cancer Biol Ther* **2,** 656–660.

[19] Livak KJ and Schmittgen TD (2001). Analysis of relative gene expression data using real-time quantitative PCR and the 2(−Delta Delta *C*(T)) method. *Methods* **25,** 402–408.

[20] Boulday G, Hamann J, Soulillou JP, and Charreau B (2002). CD97-decay–accelerating factor interaction is not involved in leukocyte adhesion to endothelial cells. *Transplantation* **73,** 429–436.

[21] Cooper CR and Pienta KJ (2000). Cell adhesion and chemotaxis in prostate cancer metastasis to bone: a minireview. *Prostate Cancer Prostatic Dis* **3,** 6–12.

[22] Morgan J, Spendlove I, and Durrant LG (2002). The role of CD55 in protecting the tumour environment from complement attack. *Tissue Antigens* **60,** 213–223.

[23] Li L, Spendlove I, Morgan J, and Durrant LG (2001). CD55 is overexpressed in the tumour environment. *Br J Cancer* **84,** 80–86.

[24] Mason JC, Lidington EA, Ahmad SR, and Haskard DO (2002). bFGF and VEGF synergistically enhance endothelial cytoprotection *via* decay-accelerating factor induction. *Am J Physiol Cell Physiol* **282,** C578–C587.

[25] Mason JC, Lidington EA, Yarwood H, Lublin DM, and Haskard DO (2001). Induction of endothelial cell decay-accelerating factor by vascular endothelial growth factor: a mechanism for cytoprotection against complement-mediated injury during inflammatory angiogenesis. *Arthritis Rheum* **44,** 138–150.

[26] Leemans JC, te Velde AA, Florquin S, Bennink RJ, de Bruin K, van Lier RA, van der Poll T, and Hamann J (2004). The epidermal growth factor–seven transmembrane (EGF-TM7) receptor CD97 is required for neutrophil migration and host defense. *J Immunol* **172,** 1125–1131.

[27] Vachino G, Gelfand JA, Atkins MB, Tamerius JD, Demchak P, and Mier JW (1991). Complement activation in cancer patients undergoing immunotherapy with interleukin-2 (IL-2): binding of complement and C-reactive protein by IL-2–activated lymphocytes. *Blood* **78,** 2505–2513.

[28] Lucas SD, Karlsson-Parra A, Nilsson B, Grimelius L, Akerstrom G, Rastad J, and Juhlin C (1996). Tumor-specific deposition of immunoglobulin G and complement in papillary thyroid carcinoma. *Hum Pathol* **27,** 1329–1335.

[29] Koretz K, Bruderlein S, Henne C, and Moller P (1992). Decay-accelerating factor (DAF, CD55) in normal colorectal mucosa, adenomas and carcinomas. *Br J Cancer* **66,** 810–814.

[30] Niculescu F, Rus HG, Retegan M, and Vlaicu R (1992). Persistent complement activation on tumor cells in breast cancer. *Am J Pathol* **140,** 1039–1043.

[31] Yamakawa M, Yamada K, Tsuge T, Ohrui H, Ogata T, Dobashi M, and Imai Y (1994). Protection of thyroid cancer cells by complement-regulatory factors. *Cancer* **73,** 2808–2817.

[32] Donin N, Jurianz K, Ziporen L, Schultz S, Kirschfink M, and Fishelson Z (2003). Complement resistance of human carcinoma cells depends on membrane regulatory proteins, protein kinases and sialic acid. *Clin Exp Immunol* **131,** 254–263.

[33] Durrant LG, Chapman MA, Buckley DJ, Spendlove I, Robins RA, and Armitage NC (2003). Enhanced expression of the complement regulatory protein CD55 predicts a poor prognosis in colorectal cancer patients. *Cancer Immunol Immunother* **52,** 638–642.

[34] Madjd Z, Durrant LG, Bradley R, Spendlove I, Ellis IO, and Pinder SE (2004). Loss of CD55 is associated with aggressive breast tumors. *Clin Cancer Res* **10,** 2797–2803.

[35] Madjd Z, Pinder SE, Paish C, Ellis IO, Carmichael J, and Durrant LG (2003). Loss of CD59 expression in breast tumours correlates with poor survival. *J Pathol* **200,** 633–639.

[36] Holla VR, Wang D, Brown JR, Mann JR, Katkuri S, and Dubois RN (2005). Prostaglandin E2 regulates the complement inhibitor CD55/decay-accelerating factor in colorectal cancer. *J Biol Chem* **280,** 476–483.

[37] Bubenik J (2004). MHC class I down-regulation: tumour escape from immune surveillance? *Int J Oncol* **25,** 487–491 (Review).

[38] Tryoen-Toth P, Vautier D, Haikel Y, Voegel JC, Schaaf P, Chluba J, and Ogier J (2002). Viability, adhesion, and bone phenotype of osteoblast-like cells on polyelectrolyte multilayer films. *J Biomed Mater Res* **60,** 657–667.

[39] Hwu P, Du MX, Lapointe R, Do M, Taylor MW, and Young HA (2000). Indoleamine 2,3-dioxygenase production by human dendritic cells results in the inhibition of T cell proliferation. *J Immunol* **164,** 3596–3599.

[40] Munn DH, Shafizadeh E, Attwood JT, Bondarev I, Pashine A, and Mellor AL (1999). Inhibition of T cell proliferation by macrophage tryptophan catabolism. *J Exp Med* **189,** 1363–1372.

[41] Grossman WJ, Verbsky JW, Tollefsen BL, Kemper C, Atkinson JP, and Ley TJ (2004). Differential expression of granzymes A and B in human cytotoxic lymphocyte subsets and T regulatory cells. *Blood* **104,** 2840–2848.

[42] Riera L, Gariglio M, Valente G, Mullbacher A, Museteanu C, Landolfo S, and Simon MM (2000). Murine cytomegalovirus replication in salivary glands is controlled by both perforin and granzymes during acute infection. *Eur J Immunol* **30,** 1350–1355.